Journal of the Korean Crystal Growth and Crystal Technology
Vol. 12, No. 6 (2002) 272-282

Mercurous bromide (Hg_2Br_2) crystal growth by physical vapor transport and characterization

S.K. Kim, S.Y. Son, K.S. Song,* J.-G. Choi and G.T. Kim*,†

Department of Chemical Engineering, Hannam University, Taejon 306-791, Korea
**Catalytic Combustion Research Center, Korea Institute of Energy Research, Taejon 305-600, Korea*

(Received August 7, 2002)
(Accepted November 18, 2002)

Abstract Mercurous bromide (Hg_2Br_2) crystals hold promise for many acousto-optic and opto-electronic applications. This material is prepared in closed ampoules by the physical vapor transport (PVT) growth method. Due to the temperature gradient between the source and the growing crystal region, the buoyancy-driven convection may occur. The effects of thermal convection on the crystal growth rate was investigated in this study in a horizontal configuration for conditions ranging from typical laboratory conditions to conditions achievable only in a low gravity environment. The results showed that the growth rate increases linearly with Grashof number, and for $0.2 \leq Ar$ (transport length-to-height, L/H) ≤ 1.0 sharply increases and for $1.0 \leq Ar \leq 20$ slowly decreases. The rate decrease exponentially with the partial pressure of component B for $Ar = 5$ and $\Delta T = 30$ K. We have also shown that the magnitude of convection decreases with the Ar. For gravity levels of less than 10^{-2} g the non-uniformity of interfacial distribution is negligible.

Key words Mercurous bromide (Hg_2Br_2), Vapor crystal growth, PVT, Convection

1. Introduction

Interest in growing Hg_2Br_2 single crystal stems from their exceptional optical properties and very broad transmission range from 0.30 to 30 μm for applications in acousto-optic and opto-electronic devices such as Bragg cells, X-ray detectors operating at ambient temperature [1]. The solid-liquid equilibrium data on the mercuric bromide ($HgBr_2$) and mercury (Hg) system has not been studied extensively. The available phase diagram [2] suggests that equimolar compound Hg_2Br_2 decomposes into two liquids at a temperature near 405°C where the vapor pressure is well above 20 atm. Because of this decomposition behavior and high vapor pressure, mercurous bromide cannot be solidified as a single crystal directly from the stoichiometric melt. However, very similar to the mercurous chloride, mercurous bromide exhibits sufficiently high vapor pressure at low temperatures so that these crystals are usually grown by the physical vapor transport (PVT) method in closed silica glass ampoules. The PVT process has many advantages over melt-growth methods since it can be conducted at relatively lower temperatures: (1) vapor-solid interfaces possess relatively high interfacial morphological stability over non-uniformities in heat and mass transfer; (2) high purity crystals can be achieved; (3) materials decomposed before melting such as Hg_2Br_2 can be grown; (4) lower point defects and dislocation densities are achieved [3]. In the PVT system of Hg_2Br_2, the molecular Hg_2Br_2 species sublimes as the vapor phase from the crystalline source material (Hg_2Br_2), and is subsequently transported and re-incorporated into the single crystalline phase (Hg_2Br_2) [4]. However, the industrial applications of the PVT process remain limited. One of the main reasons is that transport phenomena occurring in the vapor phase are quite complex and coupled so that it is difficult to design and control the process accurately. Such complexity and coupling are associated with the inevitable occurrence of thermal convection generated by the density gradients caused by the temperature gradients in the system. Thermal convection has been regarded as detrimental and, thus, to be avoided or minimized in PVT growth system. These thermal convection-induced complications result in problems ranging from crystal inhomogeneity to structural imperfection. Therefore, in order to analyze and control the PVT process accurately, and also make significant improvements in the process, it is essential to investigate the roles of thermal convection in the PVT process.

Markham, Greenwell and Rosenberger [5] examined the effects of thermal and thermosolutal convections during the PVT process inside vertical cylindrical enclosures for a time-independent system, and showed that even in the absence of gravity, convection can be present, caus-

†Corresponding author
Tel: +82-42-629-7984
Fax: +82-42-623-9489
E-mail: gtkim@mail.hannam.ac.kr

ing nonuniform concentration gradients. They emphasized the role of geometry in the analysis of the effects of convection. As such these fundamentally constitute steady state two-dimensional models. The steady state models are limited to low Rayleigh number applications, because as the Rayleigh number increases, oscillation of the flow field occurs. To address the issue of unsteady flows in PVT, Duval [6] performed a numerical study on transient thermal convection in the PVT processing of Hg_2Cl_2 very similar to the mercurous bromide for a vertical rectangular enclosure with insulated temperature boundary conditions for Rayleigh numbers up to 10^6. Duval [7] has also shown the bifurcation sequences which lead to chaotic flow in PVT processing. Nadarajah *et al.* [8] addressed the effects of solutal convection for any significant disparity in the molecular weights of the crystal components and the inert gas. Zhou *et al.* [9] reported that the traditional approach of calculating the mass flux assuming one-dimensional flow for low vapor pressure systems is indeed correct. More recently, Rosenberger *et al.* [10] studied three-dimensional numerical modeling of the PVT yielded quantitative agreement with measured transport rates of iodine through octofluorocyclobutane (C_4F_8) as inert background gas in horizontal cylindrical ampoules.

In this numerical study, a two-dimensional model is used for the analysis of the PVT processes during vapor-growth of mercurous bromide crystals (Hg_2Br_2) in horizontally oriented, cylindrical, closed ampoules in a two-zone furnace system. Mass transfer-limited processes are considered in this paper, although the recent paper of Singh, Mazelsky and Glicksman [11] demonstrated that the interface kinetics plays an important role in the PVT system of Hg_2Cl_2 very similar to the mercurous bromide. Only thermal convection will be considered at this point, primarily because the Hg_2Br_2 source materials are highly purified in the actual crystal growth process, and consequently solutally-induced convection can be ignored in comparison to thermal convection. All results presented in this paper are for a mixture of Hg_2Br_2 vapor containing some impurity, with the same molecular weight as that of Hg_2Br_2 vapor.

It is the purpose of this paper (1) to discuss the development of a mathematical model for single crystals inside a PVT reactor, incorporating the mass transfer-limited model with idealized boundary conditions, (2) to predict numerically simulated transport rate in a well characterized PVT systems over typical laboratory conditions, (3) to relate the applied convective process parameters to a crystal growth rate in order to gain insights into the underlying physicochemical processes, (4) to illustrate the possibilities of such a model in providing reactor design, parameter estimation, and process optimization.

2. Mathematical and Physical Formulation

Consider a rectangular enclosure of height H and transport length L, shown in Fig. 1. The source is maintained at a temperature T_s, while the growing crystal is at a temperature T_c, with $T_s > T_c$. PVT of the transported component A occurs inevitably, due to presence of impurities, with the presence of an inert component B; to address thermal convection we assume that the impurity B has the same molecular weight as the component A and a slight excess pressure. We also assume the sublimation and condensation of A (Hg_2Br_2) and B (Hg_2Br_2) occur congruently. The interfaces are assumed to be flat for simplicity. The finite normal velocities at the interfaces can be expressed by Stefan flow deduced from the one-dimensional diffusion-limited model [12], which provides the coupling between the fluid dynamics and species calculations. On the other hand, the tangential component of the mass average velocity of the vapor at the interfaces vanishes. Thermodynamic equilibria are assumed at the interfaces so that the mass fractions at the interfaces are kept constant at $\omega_{A,s}$ and $\omega_{A,c}$. On the horizontal non-reacting walls an appropriate velocity boundary condition is no-slip, the normal concentration gradient is zero, and temperature is imposed as a linear temperature gradient or insulated.

Thermophysical properties of the fluid are assumed to be constant, except for the density. When the Boussinesq approximation is invoked, density is assumed constant except the buoyancy body force term. The density is assumed to be a function of temperature and not of

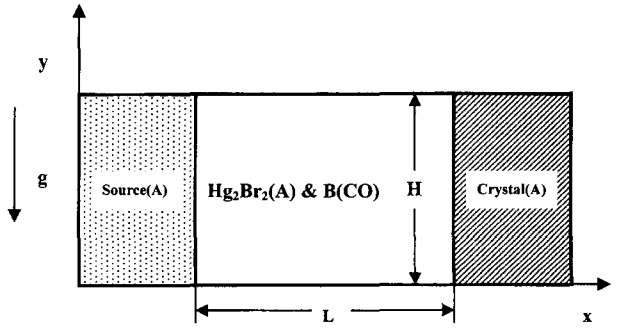

Fig. 1. Schematic of PVT growth reactor in a two-dimensional rectangular system.

concentration. The ideal gas law and Dalton's law of partial pressures are used. Viscous energy dissipation and the Soret-Dufour (thermo-diffusion) effects can be neglected, as their contributions remain relatively insignificant for the conditions encountered in our PVT crystal growth processes. Radiative heat transfer can be neglected under our conditions, based on Kassemi and Duval [13].

The transport of fluid within a rectangular PVT crystal growth reactor is governed by a system of elliptic, coupled conservation equations for mass (continuity), momentum, energy and species (diffusion) with their appropriate boundary conditions. Let u_x, u_y denote the velocity components along the x- and y-coordinates in the x, y rectangular coordinate, and let T, ω_A, p denote the temperature, mass fraction of species A (Hg_2Br_2) and pressure, respectively.

The dimensionless variables are scaled as follows:

$$x^* = \frac{x}{H},\ y^* = \frac{y}{H}, \tag{1}$$

$$u = \frac{u_x}{U_c},\ v = \frac{u_y}{U_c},\ p = \frac{p}{\rho_c U_c^2}, \tag{2}$$

$$T^* = \frac{T-T_c}{T_s-T_c},\ \omega_A^* = \frac{\omega_A-\omega_{A,c}}{\omega_{A,s}-\omega_{A,c}}. \tag{3}$$

The dimensionless governing equations are given by:

$$\nabla^* \bullet V = 0, \tag{4}$$

$$V \bullet \nabla^* V = -\nabla^* p^* + Pr\nabla^{*2} V - \frac{Gr \cdot Pr^2}{Ar^3} \cdot \frac{(1-\rho^*)}{\beta \Delta T}, \tag{5}$$

$$V \bullet \nabla^* T^* = \nabla^{*2} T^*, \tag{6}$$

$$V \bullet \nabla^* \omega_A^* = \frac{1}{Le} \nabla^{*2} \omega_A^*. \tag{7}$$

These nonlinear, coupled sets of equations are numerically integrated with the following boundary conditions:

On the walls ($0 < x^* < L/H$, $y^* = 0$ and 1):

$$u(x^*,0) = u(x^*,1) = v(x^*,0) = v(x^*,1) = 0 \tag{8}$$
$$\frac{\partial \omega_A^*(x^*,0)}{\partial y^*} = \frac{\partial \omega_A^*(x^*,1)}{\partial y^*} = 0,$$
$$T^*(x^*,0) = -\frac{1}{Ar} \cdot x^* + 1$$

On the source ($x^* = 0$, $0 < y^* < 1$):

$$u(0,y^*) = -\frac{1}{Le(Cv-1)} \frac{\partial \omega_A^*(0,y^*)}{\partial x^*}, \tag{9}$$
$$v(0,y^*) = 0,$$
$$T^*(0,y^*) = 1,$$
$$\omega_A^*(0,y^*) = 1.$$

On the crystal ($x^* = L/H$, $0 < y^* < 1$):

$$u(L/H,y^*) = -\frac{1}{LeCv} \frac{\partial \omega_A^*(L/H,y^*)}{\partial x^*}, \tag{10}$$
$$v(L/H,y^*) = 0,$$
$$T^*(L/H,y^*) = 0,$$
$$\omega_A^*(L/H,y^*) = 0.$$

The Peclet number Pe and concentration parameter Cv are defined as

$$Pe = \frac{U_{adv} L}{D_{AB}},\ C_v = \frac{1-\omega_{A,c}}{\Delta \omega}. \tag{11}$$

In the dimensionless parameters in the governing equations the thermophysical properties of the gas mixture are estimated from a gas kinetic theory using Chapman-Enskog's formulas [14]. Since the total vapor pressure can be taken to be constant during the physical vapor transport, the mass fraction of species A is defined as

$$\omega_A = \frac{1}{1+(P_T/p_A-1)M_B/M_A}. \tag{12}$$

The vapor pressure [15] p_A of Hg_2Br_2 (in the unit of Pascal) can be evaluated from the following formula as a function of temperature:

$$p_A = e^{(a-b/T)}, \tag{13}$$

In which $a = 29.75$, $b = 11767.1$. P_T denotes the total pressure, and the partial pressures for A(B) are denoted by p_A (p_B).

The crystal growth rate v_c is calculated from a mass balance at the crystal vapor interface, assuming fast kinetics, i.e. all the vapor is incorporated into the crystal, which is given by (subscripts c, v refer to crystal and vapor respectively)

$$\int \rho_v u_v \cdot ndA = \int \rho_c u_c \cdot ndA, \tag{14}$$

$$V_c = \frac{\rho_v \int u_v \cdot ndA}{\rho_c \int dA}. \tag{15}$$

In order to solve the discretization equations for the system of nonlinear, coupled governing partial differential equations, the SIMPLER (Semi-Implicit Method Pressure-Linked Equations Revised) algorithm proposed by Patankar [16] with a power law scheme was used. A 43×23 (x × y) grid system was used. The iteration procedure was continued until the following convergence criterion was satisfied:

$\left|\frac{\phi_{j+1}-\phi_j}{\phi_j}\right| < 10^{-5}$, for all ϕ,

where ϕ represents any dimensionless dependent variable being computed, e.g., u,v,T^* and ω_A^*, and j refers to the value of ϕ at the jth iteration level.

3. Results and Discussion

The parametric study is useful for showing trends and generalizing the problem, but many parameters are involved in the problem under consideration, which renders it difficult for a general analysis. One of the purposes for this study is to correlate the growth rate to process parameters for a particular material (Hg_2Br_2). Thus, it is desirable to express some results in terms of a dimensional growth rate. However, they are also applicable to parameter ranges over which the process varies in a given manner. For this application, ranges of process parameters are typical for PVT processes under ground-based laboratory conditions. The six dimensionless parameters, namely Gr, Ar, Pr, Le, C_v and Pe, are independent and arise naturally from the dimensionless governing equations and boundary conditions.

3.1. Effect of temperature gradients on growth rate

From a viewpoint of the design of a PVT crystal growth reactor, it is necessary to correlate the temperature difference between the source and crystal interfaces to the growth rate under the operating conditions examined. Figure 2 shows the growth rate of Hg_2Br_2 single crystals for various levels of temperature difference ($10 \le \Delta T \le 60$ K) in a horizontal and a vertical cylindrical reactor, based on Ar = 5, H = 2 cm, p_B = 10 torr, and T_s = 350°C. In a case of the horizontal orientation, as the temperature difference is increased from 10 K to 30 K, the growth rate increases from 0.5 to about 0.73 cm/hr, which means the rate increases by a gradient of 0.011 cm/hr/K; for $30 \le \Delta T \le 60$ K the rate decreases with a gradient of 0.0067 cm/hr/K. For the vertical case, for $10 \le \Delta T \le 30$ K, the rate increases with a gradient of 0.0073 cm/hr/K; for $30 \le \Delta T \le 60$ K the rate decreases with a gradient of 0.0027 cm/hr/K. For low temperature differences up to 30 K, the growth gradients for the horizontal case exhibit a value greater than the vertical by a factor of 1.5, while for high temperature differences from 30 through 60 K, the former is greater than the latter by a factor of 2.5. For the above cases, a maximum growth rate is obtained at around ΔT = 30 K. A maximum growth rate in the horizontal case is greater than the vertical by a factor of 1.5. At ΔT = 10 K, the growth rate in the former is greater than the latter by a factor of 1.8; at ΔT = 60 K, by a factor of 1.5. For ranges of temperature differences examined, except a low temperature difference of 10 K, a ratio of horizontal to vertical remains unchanged, i.e. a value of 1.5, which means that convective effect within the horizontal is greater than the vertical by a factor of 1.5. Moreover, the same profile of growth rate versus temperature difference, in other words, the same trend of a profile and a ratio of magnitude between both is obtained for the both cases, indicating that a convective flow pattern is likely to appear in front of the crystal region. Therefore the crystal growth rate depends significantly on the orientation of the growth reactor with respect to the gravity vector, a clear indication of a thermal buoyancy driven convective effect.

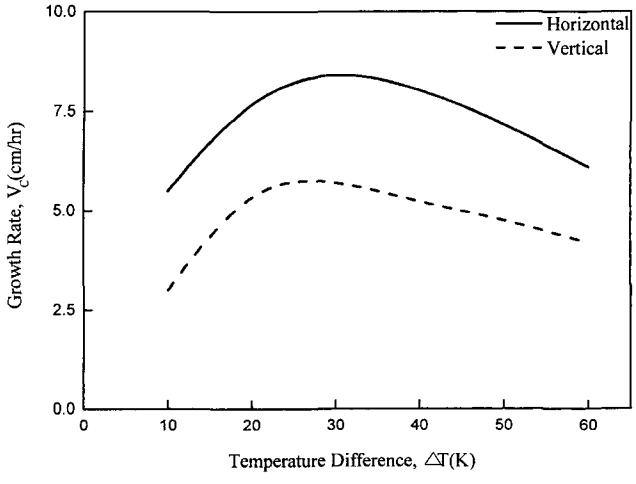

Fig. 2. Growth rate of Hg_2Br_2 as a function of temperature difference, ΔT(K) between the source and crystal for Ar = 5, H = 2 cm, P_B = 10 Torr, and T_s = 350°C. The solid line and broken lines represent the growth rate predicted by a numerical analysis based on the diffusion-limited model for the horizontal and the vertical orientation, respectively.

As seen in Fig. 2, the growth rate increases relatively linearly with increasing the temperature difference for $10 \le \Delta T \le 30$ K, while it decreases reversely with the temperature difference for $30 \le \Delta T$ 60 K. It is due to an occurrence of change in an intensity of thermal convection. To be explained in details, a Grashof number is increased with an increase in the temperature difference for the temperature ranges of $10 \le \Delta T \le 30$ K which correspond to $7.27 \times 10^6 \le Gr \le 1.14 \times 10^7$. On the other hand, for $30 \le \Delta T \le 60$ K, Grashof number decreases with increasing the temperature difference which corresponds to $1.14 \times 10^7 \ge Gr \ge 7.34 \times 10^6$ A mass fraction of a component A (Hg_2Br_2) at the source and crystal

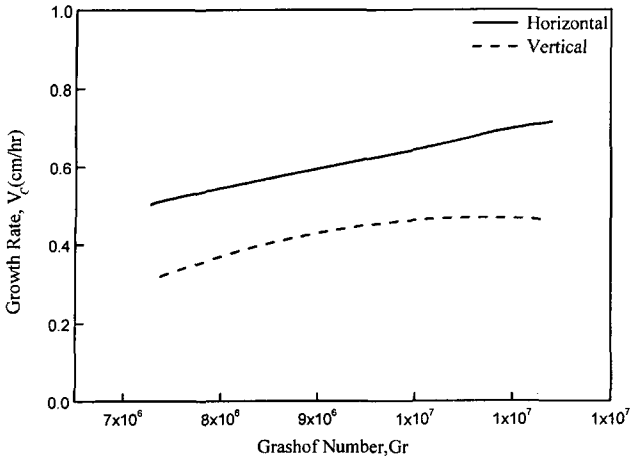

Fig. 3. Growth rate of Hg_2Br_2 as a function of Grashof number, Gr corresponding to Fig. 2.

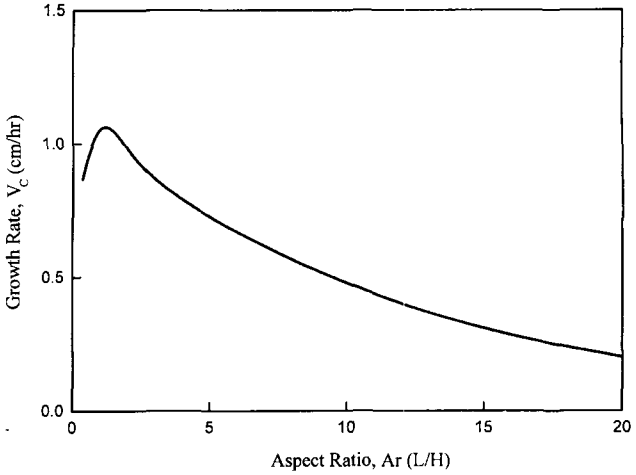

Fig. 4. Growth rate of Hg_2Br_2 as an aspect ratio, Ar (L/H) for H = 2 cm, P_B = 10 Torr, ΔT = 30 K and T_s = 350°C.

regions varies with temperatures, and thus affects the physical property of kinematic viscosity of a mixture of a component A (Hg_2Br_2) and B(CO). Thus, because in an estimation of a Grashof number for $30 \leq \Delta T \leq 60$ K, a variation in kinematic viscosity is greater than an increase in temperature difference, such a critical point as a maximum growth rate at 30 K occurs. To be clearly understood, the growth rate is plotted as a function of the intensity of thermal convection, in other words, a dimensionless Grashof number, Gr in Fig. 3 which corresponds to Fig. 2. Figure 3 shows that the growth rate increases linearly with a Grashof number for $7.27 \times 10^6 \leq Gr \leq 1.14 \times 10^7$ and that of the horizontal is greater than the vertical by a factor of 1.5. It should be noted that the ratio of 1.5 remains unchanged in either Fig. 2 or Fig. 3.

As regards to the configuration of a growth reactor, a direction of temperature gradient for the horizontal configuration is against the gravity vector, while the vertical is parallel to the gravity vector. It should be noted that thermal convection with the horizontal temperature gradient (convectional thermal convection) is fundamentally different from the case with vertical temperature gradient (thermal instability) in the sense that there is no critical thermal Rayleigh number for the occurrence of a convective cell in the presence of a horizontal temperature gradient. In general, in the vertical case as the temperature increases, multicells are formed due to thermal instability so that the intensity of thermal convection for the vertical is greater than the horizontal. However, from the viewpoint of a crystal growth rate, the crystal is grown on the diffusion-limited model so that the mass transfer in front of a crystal region for the vertical is more hindered than the horizontal.

3.2. *Effect of aspect ratio on growth rate*

The aspect ratio is one of the important process parameters, which describes the geometry of the crystal growth reactor. Experimental results [17] showed that the growth rate of mercurous halide depends on the aspect ratio (radius-to-length, R/L). These experiments did not show the detailed transport phenomena because their method was based on the determination of a mass transport crystal growth rate. In Fig. 4, the growth rate is represented as a function of aspect ratio, Ar (length-to-height, L/H) for H = 2 cm, p_B = 10 torr, T_s = 350°C, and ΔT = 30 K. Two trends are shown: the growth rate sharply increases for $0.2 \leq Ar \leq 1.0$ and slowly decreases for $1.0 \leq Ar \leq 20$. As the aspect ratio approaches a value of 20, the effects of thermal convection diminish, and the growth rate is virtually reduced to the rate predicted by an one-dimensional diffusion model. This is directly related to the fact that the cellular character of the flow field becomes less pronounced as the aspect ratio Ar is increased (not shown). In other words, this is because as the aspect ratio increases, viscous interaction with the sidewalls stabilizes thermal convection. Figure 5 shows $|U|_{max}$ as a function of an aspect ratio, Ar, corresponding to Fig. 4. As one approaches Ar = 20, i.e., the horizontal narrow enclosure, the $|U|_{max}$ decreases slowly. It is expected that the Stefan flow would occur with a further increase in aspect ratio. It has been shown [18] that the fluid flow for a horizontal rectangular system switches from a thermosolutal convective mode to a diffusive mode at Ar (transport length-to-height) = 20. This is not surprising because the effects of sidewalls tend to stabilize convection in the growth reactor. This tendency is

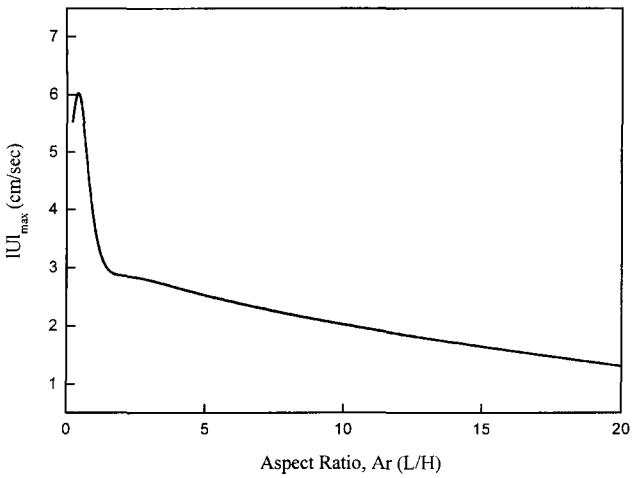

Fig. 5. $|U|_{max}$ as a function of an aspect ratio, Ar corresponding to Fig. 4, where $|U|_{max}$ as maximum magnitude of velocity vector represents an intensity of thermal convection.

consistent with the results [19-21] on pure thermal convection without crystal growth in enclosures. For aspect ratios less than Ar = 2, the $|U|_{max}$ is very sensitive to the slight change in the aspect ratio. The maximum of $|U|_{max}$ occurs for Ar = 2, beyond which there is a sharp drop, and finally levels off. This result is consistent with the results [18].

3.3. Effect of partial pressure of impurity gas on growth rate

It was found that unintentional noncondensible gas (impurity) like CO was introduced into the growth ampoules of mercurous halide due to the seal-off process [22]. Other crystal growers have also demonstrated this fact in vapor-growth experiments [23 ,24]. Generally, the presence of impurity tends to hamper or even cut off further mass transport due to the formation of a diffusion layer at the crystal interface. Consequently, the growth rate was controlled by the use of inert gas like argon. Therefore, to conclude this discussion of thermal convection in PVT crystal growth, it is of interest to examine the sensitivity of the crystal growth rate to the partial pressure of a second component.

For the study of the effect of partial vapor pressure on the growth rate, we have varied the partial pressure of component (B) assuming the same molecular weight as that of (A) ($M_A = M_B$) from 0.05 torr to 100 torr with a fixed equilibrium vapor pressure at the source temperature, T_s, of 350°C. Therefore, one considers the self-diffusion system which is encountered for high purity-materials. The addition of the B component results in an increase in total pressure, which causes the thermophysical variations of density and binary diffusion coefficient. Although the use of an inert gas along with the assumption $M_A = M_B$ would provide a better approximation of the gas mixture with impurities, our assumption represents a highly idealized system.

Assuming that the Hg_2Br_2 vapor is incompressible in the pressure ranges considered in PVT process, the binary diffusion coefficient D_{AB} is dependent on pressure, i.e., $D_{AB} \sim 1/P$. Moreover, the increase in the partial pressure of inert gas (component B) results in the decrease of mass fraction of Hg_2Br_2 at both interfaces. As a result, the mass flux is reduced. From this consideration, the addition of inert gas in PVT systems can alter the convective state. The relative contribution to mass transport (due to increase in the partial pressure) between advection and diffusion can be expressed by the Peclet number. On the other hand, the effect of thermal buoyancy-driven convection (due to increase in the partial pressure, resulting in an increase in the total pressure) is characterized by the Grashof number. This relation can be used for the rough estimation of the contribution of thermal convection, i.e., thermal Grashof number, with the increase in the total pressure. As one sees in Figs. 6 and 7, both the growth rate (shown in Fig. 6) and the $|U|_{max}$ (shown in Fig. 7) decrease exponentially with the partial pressure of component B for Ar = 5, H = 2 cm, ΔT = 30 K, and T_s = 350°C. In Figs. 6 and 7, a linear scale is chosen to demonstrate the functional relationship of the growth rate on the partial pressure of component B, p_B. This tendency was observed to be consistent with the experimental observations of Conder *et al.* [25] for a typical PVT system of mercury iodine (HgI_2) and argon, and was confirmed numeri-

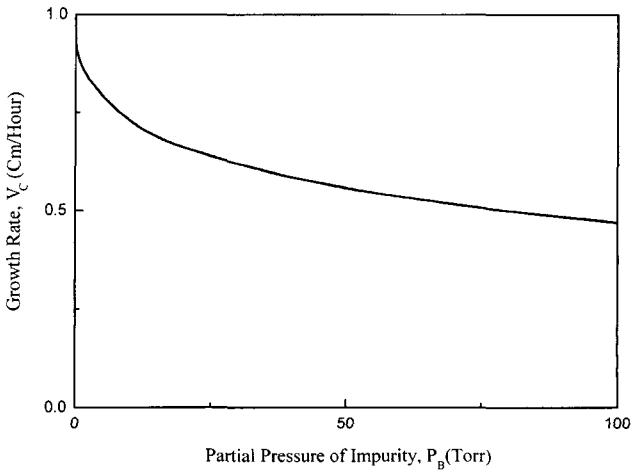

Fig. 6. Growth rate of Hg_2Br_2 as a partial pressure of impurity (CO), P_B(Torr) for Ar = 5, H = 2 cm, ΔT = 30 K and T_s = 350°C.

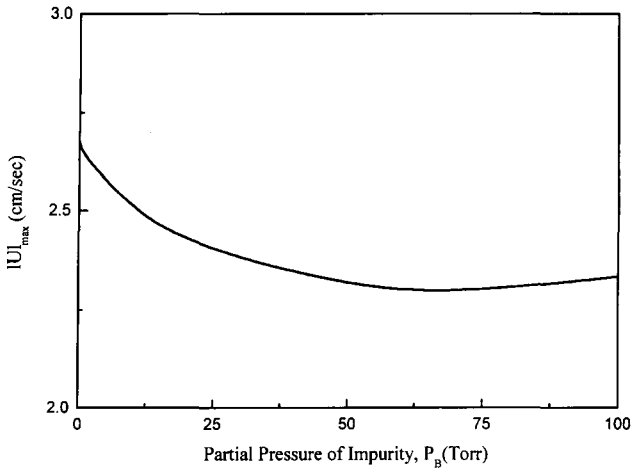

Fig. 7. $|U|_{max}$ as a partial pressure of impurity (CO), P_B(Torr) corresponding to Fig. 6.

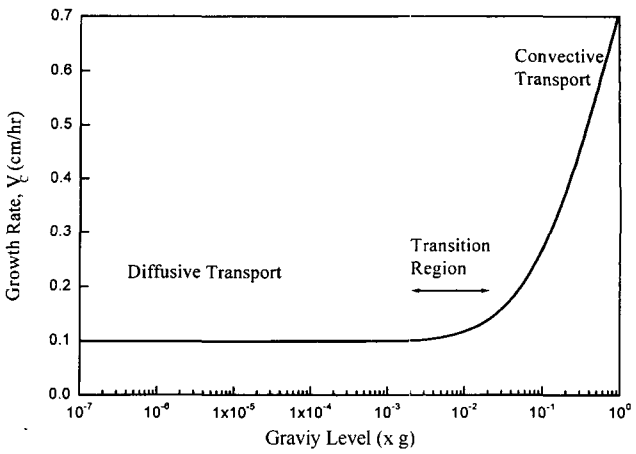

Fig. 8. Growth rate of Hg_2Br_2 as a function of gravitation level for Ar = 5, H = 2 cm, P_B = 10 Torr, ΔT = 30 K and T_s = 350°C.

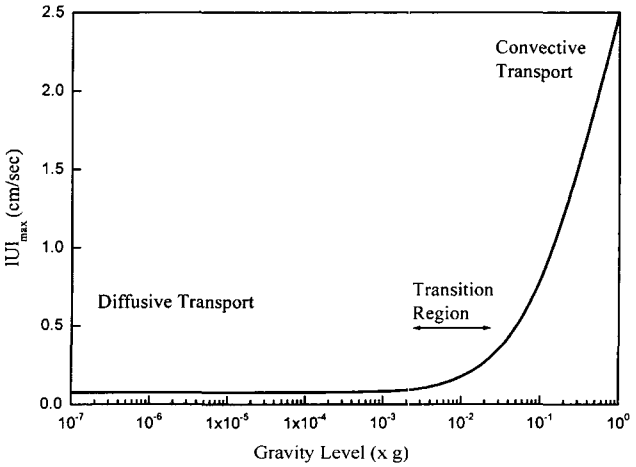

Fig. 9. $|U|_{max}$ as a function of gravitation level corresponding to Fig. 8.

cally [26] for a system of Hg_2Cl_2 and CO. Figure 6 illustrates that as the partial pressure of component B decreases from 100 torr to 0.05 torr, the rate increases by a factor of near 2 due to the intensity on convection. Moreover, with a decrease of the p_B, the $|U|_{max}$ increases due to the large sublimation and condensation velocities characterized by the Peclet number. As the total pressure decreases, the Peclet number is increased and the Grashof number is decreased slightly due to the slight variations of density. Note that for very low partial pressures of component B, the total pressure does not change, thus the Grashof number remains constant. The contribution of solutal convection to the flow (due to an increase of partial pressure) becomes important for the case when the molecular weight of the inert gas is not equal to that of the crystal component, and should be taken into account for applications to the design of a crystal growth reactor. Thus convection is aided as p_B decreases.

3.4. Effect of gravitational level on growth rate

One of the possible alternatives is to grow the crystal in a microgravity environment. The microgravity environment is of interest for research on vapor-crystal growth because buoyancy-driven convection and hydrostatic pressure can be virtually reduced or eliminated. We have simulated different levels of gravity. Figure 8 shows the sensitivity of the growth rate to the variations of the gravity level between 10^{-7} g and 1 g for a horizontal configuration with Ar = 5 and ΔT = 30 K. The effect of convection decreases with decreasing values of the gravity level, shown in Figs. 8 and 9. In particular, as the level of gravity decreases, there is a sharp decrease of a crystal growth rate near the $1g_0$ level and a much more gradual decrease thereafter.

The dimensional maximum magnitude of velocity ($|U|_{max}$) for g in Fig. 9 is 4.33 cm/s; for 0.1 g, 0.54 cm/s; for 0.01 g, 0.11 cm/s. As one sees in Fig. 9, the convective transport decreases with lower g level and is changed to the diffusive mode at 0.1 g. Therefore, for regions in which the g level is 0.1 g or less, the diffusion-driven convection results in a parabolic velocity profile and a recirculating cell does not occur (not shown). It is of interest to consider the effect of the gravitational level on interfacial distribution of a crystal growth rate, see Fig. 10. For the two gravity levels investigated, 0.1 g and 0.01 g, the interfacial distribution appear to have qualitatively a similar structure and a slight variation of growth rate over the interfacial positions, which implies that the gravitational force plays a major role in the motion of convective flow. For gravity levels of less than

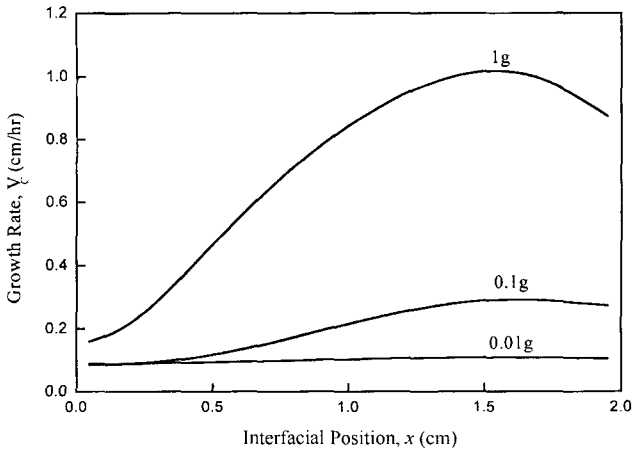

Fig. 10. Interfacial distribution of crystal growth rate for Ar = 5, H = 2 cm, P_B = 10 Torr, and T_s = 350°C for three different gravitation levels of 1 g, 0.1 g and 0.01 g.

10^{-2} g, the non-uniformity of interfacial distribution is negligible. In other words, the corresponding growth rate distribution in front of the growing interface is therefore planar. Numerical studies [10] have shown that the effect of convection can be ignored at 0.001 g or less for thermosolutal convection of Hg_2Cl_2 and CO in horizontal rectangular geometry. Even though this model does not consider the effect of solutal convection, similar trends have been achieved between the results in [13] and this investigation.

To gain insight into the effect of internal process parameters (thermophysical properties: β, κ, and ν), two cases with the same value of external process parameter $g\Delta TL^3$ are compared for the diffusion and the convection model. For example, the growth rate for 0.1 g with ΔT = 30 K and Ar = 5 is compared with the rate for 1 g, ΔT = 3 K, and Ar = 5. The former has the growth rate of 0.2 cm/hr (at $Gr = 1.14 \times 10^6$, Pr = 1.31, Le = 0.39, C_v = 1.02, Pe = 4.03), whereas the latter has the rate of 0.16 cm/hr (for $Gr = 2.65 \times 10^6$, Pr = 1.05, Le = 0.30, C_v = 1.27, Pe = 1.55). Thus, the former rate is a little greater than the latter since the former has the Peclet number by a factor of 2.6 higher and the Grashof number by a factor of 2.3 lower than the latter. The increase in Peclet number and decrease in Grashof number are due to the fact that the crystal temperature T_c for the former case is lower than for the latter and, thus, the mean temperature T_0 and mass fraction $\omega_{A,0}$ for the former case is smaller than the latter. Note that for the PVT processes examined, the source temperature T_s is fixed at 350°C and the crystal temperature T_c is decreased as ΔT increases. Therefore, an increase in Peclet number due to the mean operating temperature would be offset by a decrease in Grashof number so that the corresponding resulting growth rates are nearly the same. But, property variations due to the mean operating temperature affect significantly the governing parameters such as Grashof and Peclet numbers, which would determine the strength of thermal convection.

3.5. Effect of wall thermal boundary conditions on growth rate

For practical applications, it is sometimes necessary to insulate the region near the walls to prevent spontaneous nucleation of crystals on the walls. We thus consider insulated boundaries and illustrate the difference between the insulated and conducted wall boundaries. For the operating conditions studied, the numerical convergence for the conducting cases is not readily achieved compared with the insulating cases. One explanation is that the energy used to drive the thermal convection can not escape through the insulating walls so that the convection motion for the insulating case is more stable than the conducting case. Figure 11 shows that the growth rate of Hg_2Br_2 as a function of temperature difference, ΔT (K) between the source and crystal for Ar = 5, H = 2 cm, P_B = 10 Torr, and T_s = 350°C with two different temperature wall boundary conditions, i.e., conducting and insulating walls. The rate of the insulating walls for $10 \le \Delta T \le 60$ K is greater than that of the conducting walls. Thus, the rate is significantly governed by a diffusion mode in front of the crystal region for the horizontal configuration. However, as shown in Fig. 12,

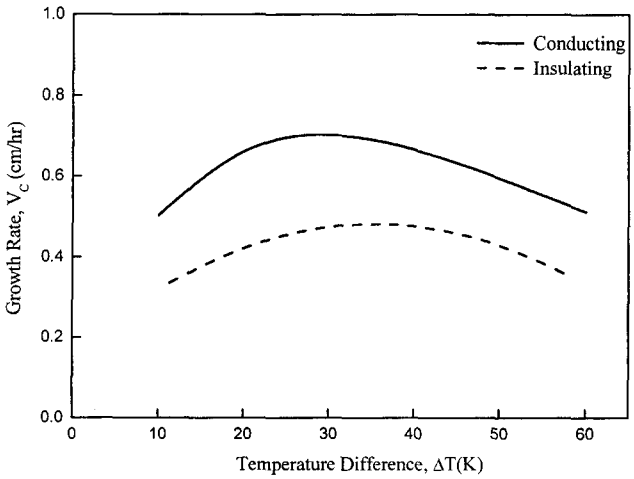

Fig. 11. Growth rate of Hg_2Br_2 as a function of temperature difference, ΔT (K) between the source and crystal for Ar = 5, H = 2 cm, P_B = 10 Torr, and T_s = 350°C with two different temperature wall boundary conditions, i.e., conducting and insulating walls.

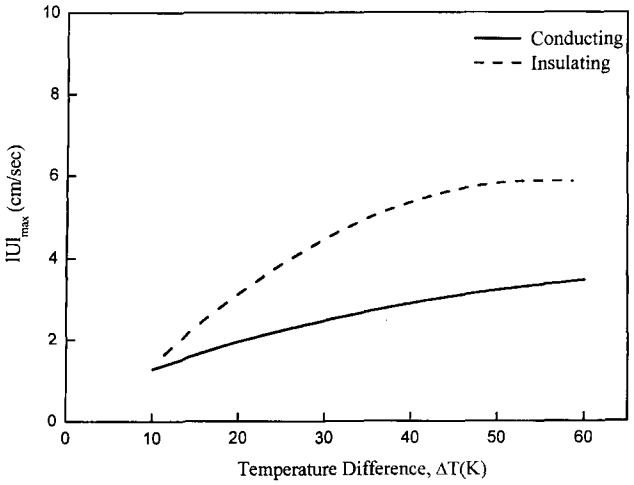

Fig. 12. $|U|_{max}$ as a function of temperature difference, ΔT (K) corresponding to Fig. 11, where $|U|_{max}$ as maximum magnitude of velocity vector represents an intensity of thermal convection.

for $Ar = 5$ and $7.27 \times 10^6 \leq Gr \leq 1.14 \times 10^7$, $|U|_{max}$ for the conducting case is greater than the insulating. The reason for the lower magnitude of flow velocity is that the insulating wall case has a diffusion-dominant mode, while the conduction wall case is of a convective mode. Note that $|U|_{max}$ is indicative of thermal convective magnitude of flow field and is not directly proportional to the rate.

4. Conclusions

In the past years considerable progress has been achieved in modeling PVT processes. Our study covers the effects of thermal convection on the growth rate of Hg_2Br_2 crystals in a rectangular ampoule under terrestrial and micro-gravitational conditions for various operating parameters. Taking into account the real thermodynamical dependency of the mass fraction as a function of temperature reduces considerably the control we have on the process. The growth rate and convective magnitude of PVT were studied by isolating the trends of thermal convection form the combination of thermo-solutal convection. We studied thermal convection by artificially eliminating solutal convection, i.e., by setting the masses of both gas components equal. Our results show that the growth rate increases linearly with Grashof number for $7.27 \times 10^6 \leq Gr \leq 1.14 \times 10^7$, and for aspect ratios, $0.2 \leq Ar \leq 1.0$ sharply increases and for $1.0 \leq Ar \leq 20$ slowly decreases. The rate decrease exponentially with the partial pressure of component B for $Ar = 5$ and $\Delta T = 30$ K. We have also shown that the magnitude of convection decreases with the aspect ratio (Ar). The growth rate for the horizontal configuration.is greater than the vertical configuration. The vertical configurations would provide potential for a diffusive mode of transport of mass, resulting in a uniform mass flux near the interface (planar growth). Microgravity appears to be an efficient way of resolving the problems. The magnitude of convection varies approximately with the gravitational acceleration, as does the interfacial distribution on the growing interface. For gravity levels of less than 10^{-2} g, the convective mode switches to a diffusive mode, associated with a restored planar growth. and the non-uniformity of interfacial distribution is negligible because the Stefan wind drives the flow. Buoyancy-driven convection in PVT is almost unavoidable at 1-g because of the density gradients which are omnipresent. What are the possible actions at 1-g? Two actions come to our mind: Firstly, choice of the buffer gas: most of our problems arise from the huge difference in molar mass between carbon mono-oxide and mercurous bromide. Secondly, we could use a heavier gas. We can change the geometry of the ampoule, using the conclusion of the study of the effect of the aspect ratio (narrow ampoule). Alternatively, the following may also be possible: we can modify the partial pressure of the components. Increasing the partial pressure of component B would reduce convection, but also reduce the rate of growth, the diffusion coefficient decreasing with pressure. Decreasing the reactor total pressure by decreasing the partial pressure of an inert component increases the diffusion transfer, which leads to the increase of the Peclet number. Also, because the addition of inert gas causes a decrease of thermal convection (Grashof number) due to the variation of the vapor density, its contribution to the flow should be taken into account for the design of a crystal growth reactor.

Acknowledgement

This work was supported by Korea Research Foundation Grant (KRF-1999-Sundo E00402).

Nomenclature

A : component A, Hg_2Br_2
B : component B, CO
D_{AB} : diffusivity of A and B
g : standard gravitational acceleration constant, 980.665

cm/s^2

H : height (cm)
L : transport length, width (cm)
M : mean molecular weight of component A and B
P : pressure
P_T : total pressure
T : temperature
ΔT : temperature difference between source and crystal, $T_s - T_c$
$\Delta\omega$: mass fraction difference between source and crystal, $\omega_{A,s} - \omega_{A,c}$
x : x-coordinate
y : y-coordinate
u : dimensionless x-component velocity
U_{adv} : characteristic velocity based on the diffusive-advective flux
U_c : characteristic velocity, k/H
$|U|_{max}$: dimensional maximum magnitude of velocity vector (cm/s)
v : dimensionless y-component velocity
u_x : x-component velocity
u_y : y-component velocity
V : velocity vector
V_c : growth rate (cm/hr)

Dimensionless Governing Parameters

Ar : aspect ratio, L/H
C_v : concentration parameter, $C_v = (1-\omega_{A,c})/\Delta\omega$
Le : Lewis number, κ/D_{AB}
Pe : Peclet number, $U_{adv}L/D_{AB}$
Pr : Prandtl number, ν/κ
Gr : Grashof number, $g\beta\Delta TL^3/\nu^2$

Subscripts and Superscripts

A : component A, Hg_2Br_2
Adv : advection
B : component B, CO
c : crystal
s : source
T : total vapor pressure
* : dimensionless

Greek Letters

β : thermal volume expansion
κ : thermal diffusivity
ν : kinematic viscosity
∇^* : $(\partial/\partial x^*) + (\partial/\partial y^*)$
∇^{*2} : $(\partial^2/\partial x^{*2}) + (\partial^2/\partial y^{*2})$
ϕ : variable (u, v, T*, ω_A^*)
ω : mass fraction meaning dimensionless mass concentration
ρ : density of fluid with component A and B

References

[1] N.B. Singh *et al.*, "Growth and Characterization of Mercurous Halide Crystals:mercurous Bromide System", J. Crystal Growth 137 (1994) 155.
[2] Dworsky and K. Komarek, Monatsh. Chem. 101 (1970) 976.
[3] F. Rosenberger, "Fluid Dynamics in Crystal Growth from Vapors", Physico-Chemical Hydro-dynamics 1 (1980) 3.
[4] N.B. Singh *et al.*, "Mercurous Bromide Acousto-optic Devices", J. Crystal Growth 89 (1986) 173.
[5] B.L. Markham, D.W. Greenwell and F. Rosenberger, "Numerical Modeling of Diffusive-convective Physical Vapor Transport in Cylindrical Vertical Ampoules", J. Crystal Growth 51 (1981) 426.
[6] Walter M.B. Duval, "Convection in the Physical Vapor Transport Process-- I: Thermal", J. Chemical Vapor Deposition 2 (1994) 188.
[7] Walter M.B. Duval, "Transition to Chaos in the Physical Transport Process--I", *the Proceeding of the ASME--WAM Winter Annual meeting, Fluid mechanics phenomena in microgravity*, ASME-WAM, New Orleans, Louisiana, Nov. 28 -- Dec. 3, AMD-174, FED-175 (1993) 51.
[8] A. Nadarajah, F. Rosenberger and J. Alexander, "Effects of Buoyancy-driven Flow and Thermal Boundary Conditions on Physical Vapor Transport", J. Crystal Growth, 118(1992) 49.
[9] H. Zhou, A. Zebib, S. Trivedi and W.M.B. Duval, "Physical Vapor Transport of Zinc-telluride by Dissociative Sublimation", J. Crystal Growth 167 (1996) 534.
[10] F. Rosenberger, J. Ouazzani, I. Viohl and N. Buchan, "Physical Vapor Transport Revised", J. Crystal Growth 171 (1997) 270.
[11] N.B. Singh, R. Mazelsky and M.E. Glicksman, "Evaluation of Transport Conditions During PVT: Mercurous Chloride System", PhysicoChemical Hydrodynamics 11(1) (1989) 41.
[12] F. Rosenberger and G. Muller, "Interfacial Transport in Crystal Growth, a Parameter Comparison of Convective Effects", J. Crystal Growth 65 (1983) 91.
[13] M. Kassemi and Walter M.B. Duval, "Interaction of Surface Radiation with Convection in Crystal Growth by Physical Vapor Transport", J. Thermophys. Heat Transfer 4 (1989) 454.
[14] R.B. Bird, W.E. Stewart and E.N. Lightfoot, "Transport Phenomena" (New York, NY: John Wiley and Sons, 1960).
[15] H. Oppermann, "Chemical Aspects of Hg_2X_2-Decomposition, Barogram-diagram and Thermodynamic Data", Proceedings of the 2nd Intl symposium on univalent mercury halides, Czecoslovakia (1989).

[16] S.V. Patankar, "Numerical Heat Transfer and Fluid Flow" (Washington D. C.: Hemisphere Publishing Corp., 1980).
[17] N.B. Singh, M. Gottlieb, R.H. Hopkins, R. Mazelsky, W.M.B. Duval and M.E. Glicksman, "Physical Vapor Transport Growth of Mercurous Chloride Crystals", *Prog. Crystal Growth and Charact.* 27 (1993) 201.
[18] Christopher Mennetrier and Walter M.B. Duval, "Thermal-solutal Convection with Conduction Effects Inside a Rectangular Enclosure", NASA TM 105371 (1991).
[19] I. Catton and D.K. Edwards, "Effects of Side Walls on Natural Convection Between Horizontal Plates Heated from Below", J. Heat Transfer 89 (1967) 295.
[20] D.K. Edwards, "Suppression of Cellular Convection by Lateral Walls", J. Heat Transfer 91 (1972) 145.
[21] I. Catton, "Effect of Wall Conducting on the Stability of a Fluid in a Rectangular Region Heated from Below", J. Heat Transfer 94 (1972) 446.
[22] N.B. Singh, G. Marshall, M. Gottlieb, G.B. Brandt, R.H. Hopkins, R. Mazelsky, Walter M.B. Duval and M.E. Glicksman, "Purification and Characterization of Mercurous Halides", J. Crystal Growth 106 (1990) 61.
[23] G.J. Russell and J. Woods, "The Growth of CdS in Sealed Silica Capsules", J. Crystal Growth 46 (1979) 323.
[24] J.R. Cutter and J. Woods, "Growth of Single Crystals of Zinc Selenide from the Vapor Phase", J. Crystal Growth 47 (1979) 405.
[25] K. Conder, J. Przyluski and J. Laskowski, "Vapor Transport Rate of HgI_2 in the Presence of Inert Gas", J. Crystal Growth 74 (1986) 416.
[26] Christophe Mennetrier and Walter M.B. Duval, "Physical Vapor Transport of Mercurous Chloride Under a Nonlinear Thermal Profile", NASA TM 105920 (1992).